Using surface markers for MRI guided breast conserving surgery: a feasibility survey

2014 Phys. Med. Biol. 59 1589

(http://iopscience.iop.org/0031-9155/59/7/1589)

IOP Publishing | Institute of Physics and Engineering in Medicine Physics in Medicine and Biology

Phys. Med. Biol. **59** (2014) 1589–1605 doi:10.1088/0031-9155/59/7/1589

Using surface markers for MRI guided breast conserving surgery: a feasibility survey

Mehran Ebrahimi[1], **Peter Siegler**[2], **Amen Modhafar**[2], **Claire M B Holloway**[3], **Donald B Plewes**[4] **and Anne L Martel**[2,4]

[1] Faculty of Science, University of Ontario Institute of Technology, 2000 Simcoe St N, Oshawa, ON, Canada, L1H 7K4
[2] Imaging Research, Sunnybrook Research Institute, 2075 Bayview Avenue, Toronto, ON, Canada, M4N 3M5
[3] Department of Surgery, Sunnybrook Health Sciences Centre, 2075 Bayview Avenue, Toronto, ON, Canada, M4N 3M5
[4] Department of Medical Biophysics, University of Toronto, Toronto, ON, Canada

E-mail: mehran.ebrahimi@uoit.ca

Received 4 March 2013, revised 20 December 2013
Accepted for publication 4 February 2014
Published 10 March 2014

Abstract

Breast MRI is frequently performed prior to breast conserving surgery in order to assess the location and extent of the lesion. Ideally, the surgeon should also be able to use the image information during surgery to guide the excision and this requires that the MR image is co-registered to conform to the patient's position on the operating table. Recent progress in MR imaging techniques has made it possible to obtain high quality images of the patient in the supine position which significantly reduces the complexity of the registration task. Surface markers placed on the breast during imaging can be located during surgery using an external tracking device and this information can be used to co-register the images to the patient. There remains the problem that in most clinical MR scanners the arm of the patient has to be placed parallel to the body whereas the arm is placed perpendicular to the patient during surgery. The aim of this study is to determine the accuracy of co-registration based on a surface marker approach and, in particular, to determine what effect the difference in a patient's arm position makes on the accuracy of tumour localization. Obtaining a second MRI of the patient where the patient's arm is perpendicular to body axes (operating room position) is not possible. Instead we obtain a secondary MRI scan where the patient's arm is above the patient's head to validate the registration. Five patients with enhancing lesions ranging from 1.5 to 80 cm^3 in size were imaged using contrast enhanced MRI with their arms in two

positions. A thin-plate spline registration scheme was used to match these two configurations. The registration algorithm uses the surface markers only and does not employ the image intensities. Tumour outlines were segmented and centre of mass (COM) displacement and Dice measures of lesion overlap were calculated. The relationship between the number of markers used and the COM-displacement was also studied. The lesion COM-displacements ranged from 0.9 to 9.3 mm and the Dice overlap score ranged from 20% to 80%. The registration procedure took less than 1 min to run on a standard PC. Alignment of pre-surgical supine MR images to the patient using surface markers on the breast for co-registration therefore appears to be feasible.

Keywords: image registration, thin-plate spline, breast MRI, image guided surgery

(Some figures may appear in colour only in the online journal)

1. Introduction

Dynamic contrast enhanced (DCE) MRI provides a very high sensitivity for the detection of breast cancer (Peters *et al* 2008) and a sharp delineation of breast lesions (Goto *et al* 2007, DeMartini *et al* 2008). It is therefore a good choice of imaging modality to aid the surgeon when performing breast conserving surgery (BCS). The surgeon will typically use the MR images to review the size and location of the tumour before making the first incision in order to minimize the amount of tissue excised whilst still ensuring that clear surgical margins are achieved. However, breast MRI is commonly performed in the prone position where the breasts are pendant into the imaging coils and even immobilized by slight pressure from the coils or fixation plates (Konyer *et al* 2002, Piron *et al* 2003). This configuration differs significantly from the situation found in operating room (OR) during BCS, where the patient is in the supine position with the breast remaining in its native configuration. This different patient positioning hinders the use of breast MRI for image guidance of BCS (Carter *et al* 2006, 2008) as the surgeon has to mentally correct for the differences in orientation.

To overcome this restriction, breast MRI in the supine position has been proposed (Alderliesten *et al* 2010). In one approach (Siegler *et al* 2011) the patient is placed on her back on the MR bed while a fixture holds the imaging coil above the breast of the patient. In this setting, the breast is not constrained or compressed in any form during imaging. It therefore falls into its native configuration, which is expected to be closer to that in the OR setting than is the case with prone imaging. However, in most clinical MR scanners the arm of the patient has to be placed parallel to the body, whereas the arm is placed perpendicular to body axes during surgery. Since soft breast-tissue is inhomogeneous and anisotropic (Guo *et al* 2006), a positional change of the arm will cause a non-rigid-body deformation of the adjacent breast.

In order to correct for changes in breast conformation that occur due to different patient positions during imaging and at surgery, image registration is required. In the OR it is not practical to carry out 3D breast imaging (MRI, CT, or ultrasound) therefore a registration method needs to be based on the alignment of surface information only (see figure 1). It also needs to be fast in order to minimize the delay whilst the patient is under anasthesia. A surface based technique, which uses MR markers and pen markings together with optical tracking to detect certain points on the breast skin, satisfies both of these constraints.

The aim of this study is to determine whether a surface marker based deformable registration method is able to correct for changes in breast conformation and correctly locate

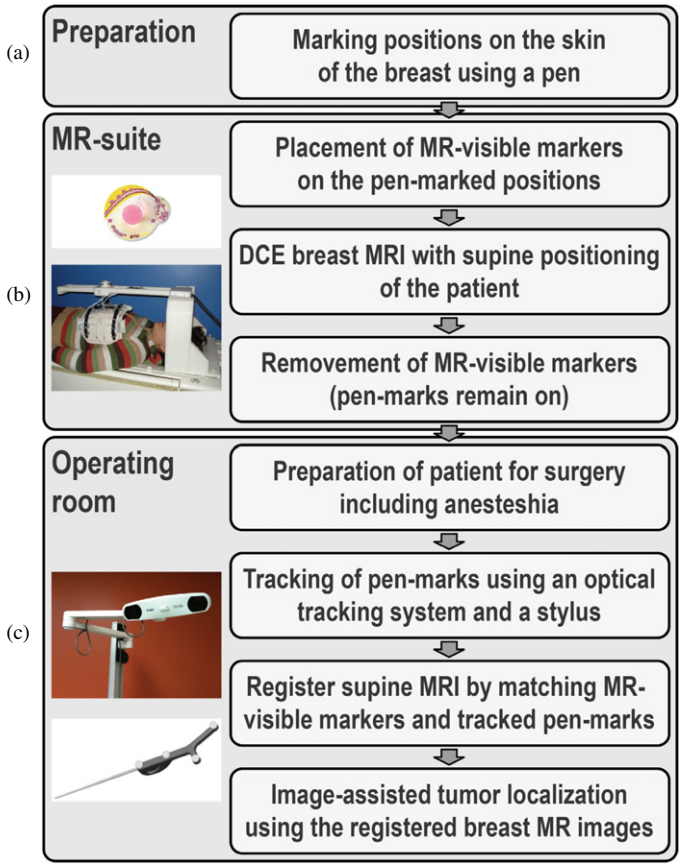

Figure 1. Flowchart of the suggested image-assisted BCS based on supine breast MRI. (a) On the day of the surgery, certain positions on the skin of the beast are marked with a suitable pen. (b) Before the MRI, MRI-visible markers are placed on the marked positions. The MRI-coordinates of the markers inside the acquired 3D supine MR data sets are recorded. After the MRI, the MRI-markers are removed from the breast leaving only the pen-marks on the breast skin. (c) In the OR the patient is prepared for surgery, which includes the placing on the surgical bed and the application of anesthesia. The pen-marked positions are tracked using an optical tracking system and a stylus pointing device. Then the supine MRI are registered to the OR using the positions of the MR-visible markers inside the 3D images and the tracked positions of the pen-marks in the OR.

the tumour location within the breast. Ideally, accuracy would be assessed by carrying out the full procedure illustrated in figure 1 to align the pre-surgical images with the patient in the OR. This is not practical however, as there is no way of measuring the location of the tumour and hence the centre of mass (COM)-displacement without imaging. The OR part of the procedure is replaced with a second MRI scan carried out after repositioning the patient in the scanner with a different arm position. Obtaining a second MRI of the patient where the patient's arm is perpendicular to body axes (OR position) is not possible. Instead we obtain a secondary MRI scan where the patient's arm is above the patient's head. The assumption is that the tissue displacement from the arm-parallel position is greater in this secondary scan (arm-above) compared to the actual OR position (arm-perpendicular). If the registration is feasible

between the arm-above and arm-parallel positions then it is also feasible for the arm-above and arm-perpendicular positions. Therefore for our validation we consider the arm-parallel and arm-above position image volumes for which we can obtain MRI scans.

The result of the registration between these two image volumes provides a surrogate measure of the tumour localization accuracy during surgery. There are an overwhelming number of registration methods known in the literature, which might be used for this problem. See, e.g., the books (Highnam and Brady 1999, Hajnal *et al* 2001, Rohr 2001, Toga and Thompson 2001, Modersitzki 2004, Yoo 2004, Goshtasby 2005, Scherzer 2006, Modersitzki 2009) and references therein.

A marker based thin-plate spline (TPS) (Duchon 1976, Bookstein 1989) registration scheme was selected to align the supine breast MRI data with the breast position of the patient in the OR as it is very fast, a necessary characteristic since the registration will be carried out whilst the patient is under anaesthesia.

In this paper, the accuracy of the TPS registration will be tested and effect of varying the number of surface markers and their position on the breast on the registration error will be assessed.

2. Materials and methods

2.1. The thin-plate spline (TPS) registration scheme

In this section, a detailed description of the TPS landmark-based registration is presented. The idea of TPSs was initially introduced by the pioneering work of Duchon (Duchon 1976) and was later employed for image registration, see e.g., (Modersitzki 2009) and the articles within.

Let $t_j = [t_j^1, t_j^2, t_j^3]$ denote the position of the jth landmark located during surgery (in this study this is taken to be the location of the markers in the arm up image) and $r_j = [r_j^1, r_j^2, r_j^3]$ the position of the corresponding landmark in the pre-surgical image, $j = 1, \ldots, n$, where n is the number of given landmarks. The goal is to find the transformation $y : \mathbb{R}^3 \to \mathbb{R}^3$, such that

$$y(r_j) = t_j \quad \text{for all} \quad j = 1, \ldots, n, \tag{1}$$

which minimizes the objective function

$$S[y] = \int_\Omega \sum_{i,p,q=1}^{3} [\partial_{p,q} y^i(x)]^2 \, \mathrm{d}x. \tag{2}$$

This is the linearized bending energy of a thin plate in 3D that imposes some kind of smoothness on y. It has been shown (Duchon 1976) that the solution of component y^i of the unknown transformation y belongs to a certain space that is spanned by shifts of an *a-priori* known function and a polynomial correction term. To be precise, in 3D

$$y^i(x) = \sum_{j=1}^{n} c_j^i \|x - r_j\| + w_0^i + w_1^i x^1 + w_2^i x^2 + w_3^i x^3, \quad i = 1, \ldots, 3. \tag{3}$$

Fortunately the solution can be obtained by solving a linear system of equations to evaluate the coefficients of this expression. If we define $A = [\|r_k - r_j\|] \in \mathbb{R}^{n,n}$, $t^i = [t_1^i, t_2^i \ldots, t_n^i]^T \in \mathbb{R}^{n,1}$, $c^i = [c_1^i, c_2^i \ldots, c_n^i]^T \in \mathbb{R}^{n,1}$, $w^i = [w_0^i, w_1^i, w_2^i, w_3^i]^T \in \mathbb{R}^{4,1}$ and $B = [e, r] \in \mathbb{R}^{n,4}$, where $e = [1, \ldots, 1]^T \in \mathbb{R}^{n,1}$, $r = [r_j^i] \in \mathbb{R}^{n,3}$, the landmark correspondence and the transformation energy minimization condition yields

$$\begin{bmatrix} A & B \\ B^T & 0_{4,4} \end{bmatrix} \begin{bmatrix} c^i \\ w^i \end{bmatrix} = \begin{bmatrix} t^i \\ 0_{4,1} \end{bmatrix} \tag{4}$$

for $i = 1, \ldots, 3$, see (Modersitzki 2009).

Table 1. Characteristics of patient datasets.

Patient ID	Matrix size	Field of view (mm^3)	no. of markers arm down, up and matched	Tumour size arm down (cm^3)	Tumour size arm up (cm^3)
1	$256 \times 256 \times 66$	$180 \times 180 \times 79$	34, 33, 33	16.8 ± 0.4	18.0 ± 1.1
2	$256 \times 256 \times 56$	$190 \times 190 \times 84$	40, 29, 24	5.3 ± 0.7	6.9 ± 1.0
3	$256 \times 256 \times 66$	$240 \times 240 \times 79$	34, 35, 34	80.5 ± 4.1	73.8 ± 1.6
4	$256 \times 256 \times 72$	$200 \times 200 \times 86$	24, 24, 24	2.4 ± 0.1	2.4 ± 0.4
6	$256 \times 256 \times 46$	$200 \times 200 \times 55$	25, 25, 25	1.9 ± 0.2	1.5 ± 0.2

Hence, by substituting the evaluated coefficients c^i, w^i we can determine y^i as well as the desired unknown transformation y.

Note that in evaluating the transformation y, we only use the location information of the landmarks in the pre-surgical image and the corresponding locations during the surgery. Therefore, no image intensity information is required in the registration procedure. However in our feasibility study, we use the image intensity information to evaluate the location of the markers in the two images. Furthermore, we use the image intensities when we transform and compare the 3D intensity volumes in the validation step. This is required to yield a surrogate measure of the tumour localization accuracy during surgery.

2.2. Acquisition of a test dataset

Patients with a previously detected enhancing lesion on MRI who were waiting for surgery were approached to participate in the study. Approval for the study was obtained from the Institutional Ethics Board and over the period of one year six volunteers were recruited.

Immediately before imaging a range of 24–34 MR visible markers (Brava-Pinpoint, Beekley, USA) were placed on the skin of the left breast in a uniform distribution for each volunteer, see table 1. The markers were held with stickers to the breast skin and, in order to minimize disturbances in the natural behaviour of the breast during the arm movement, these stickers were trimmed to achieve as small a contact surface as possible.

Supine breast MRI was performed on a whole body 1.5T MR scanner (GE Signa Excite). After obtaining informed consent, unilateral scans were acquired from the left breasts of the free-breathing patient volunteers using the supine breast apparatus and a fast 3D spoiled gradient echo sequence (oblique coronal slice orientation, frequency encoding from left to right, TE = 4.2 ms, TR = 16.2 ms, flip-angle = 30°) with fat saturation (Siegler *et al* 2011). Table 1 summarizes characteristics of the obtained datasets for five patients.

It should be noted that some of the markers occasionally fell off during the process of repositioning. In addition, there is no guarantee that by moving the patient, all of the markers remain in the field of view of the image volume in the moving image compared to the fixed image. The difference between the number of markers in these two cases especially for patient no. 2 is a combined consequence of these two events. Patient no. 5 was coughing throughout the scanning procedure leading to unacceptably poor quality images in which it was impossible to delineate the tumour; the data from this patient is therefore not included in the study.

The patients were initially positioned in the supine position with their arms by their sides and contrast was injected in the contralateral (right) arm. After acquiring the first contrast enhanced image the patients were then quickly repositioned for the second supine breast MRI with the arm placed above the head.

The performance of the TPS registration was evaluated using the two supine MR images of the breast, where the arm in the so-called reference image is in the parallel position and is outstretched in the so-called arm up image, see figures 2, 3.

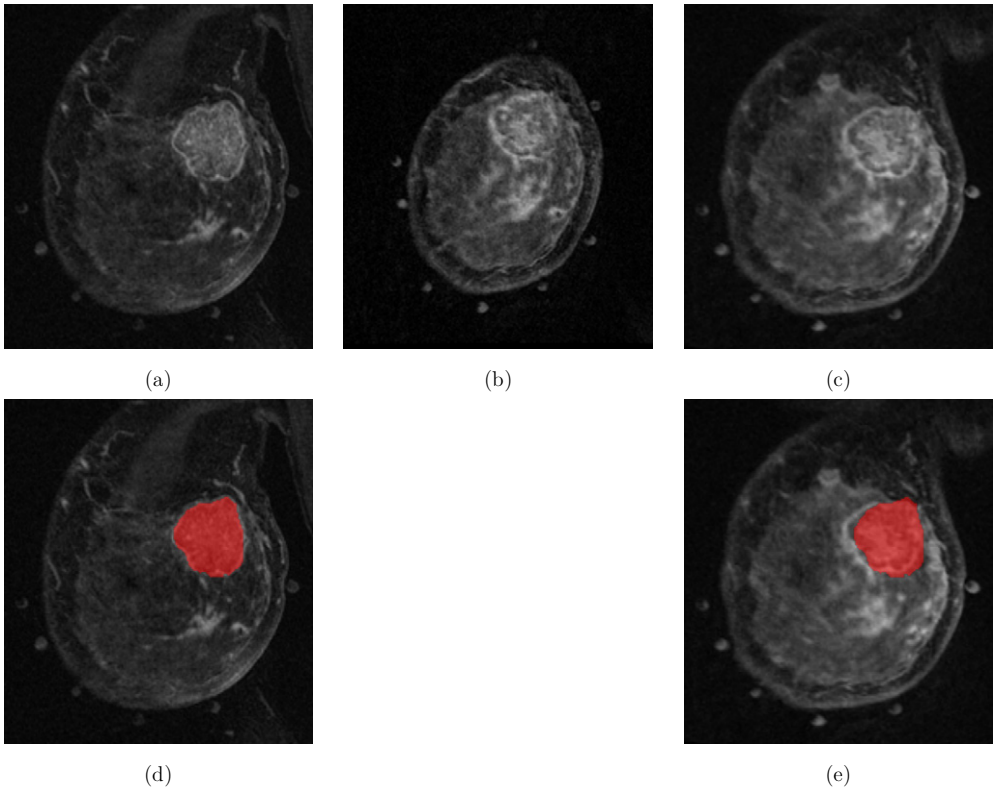

Figure 2. Images with (a) the arm adjacent to the body (reference) and (b) the arm placed above the head (arm up). Result of the registration of the arm up to the arm down (c). Segmented tumour in the arm down image (d) shown in red and as a colour-overlay on the registered image (e).

2.3. Marker selection and matching

The position of the MR-visible markers in the two images were semi-manually selected and computed using a GUI tool that we developed inhouse using MATLAB. An algorithm, which offers a simultaneous TPS registration and an automatic marker matching (Chui and Rangarajan 2003) was then employed to match the markers.

The matching procedure required a set of parameters introduced in Chui and Rangarajan (2003). We manually tuned the parameters for the algorithm to yield accurate matching of the markers in a volunteer dataset. In our experiments, we used the default `cMIX` function of the robust point matching (RPM) package available at http://noodle.med.yale.edu/~chui/tps-rpm.html. Initially, the marker position coordinates were rescaled by a factor of 500. This ensured the position coordinates were in the interval [0, 1] consistent with the examples used in the RPM package demo to avoid any possible instabilities. We used the parameters `frac`, `T_init`, and `T_finalfac` respectively as 1, 0.5 and 500 as it was defined in the `cMIX` function of RPM package demo. The annealing rate was set as 0.90 in the `cMIX` code. We then called `cMIX(Fposition, Mposition, frac, T_init, T_finalfac)` in which `Fposition` and `Mposition` were respectively the rescaled marker positions in the fixed and moving images. The matching procedure on the volunteer

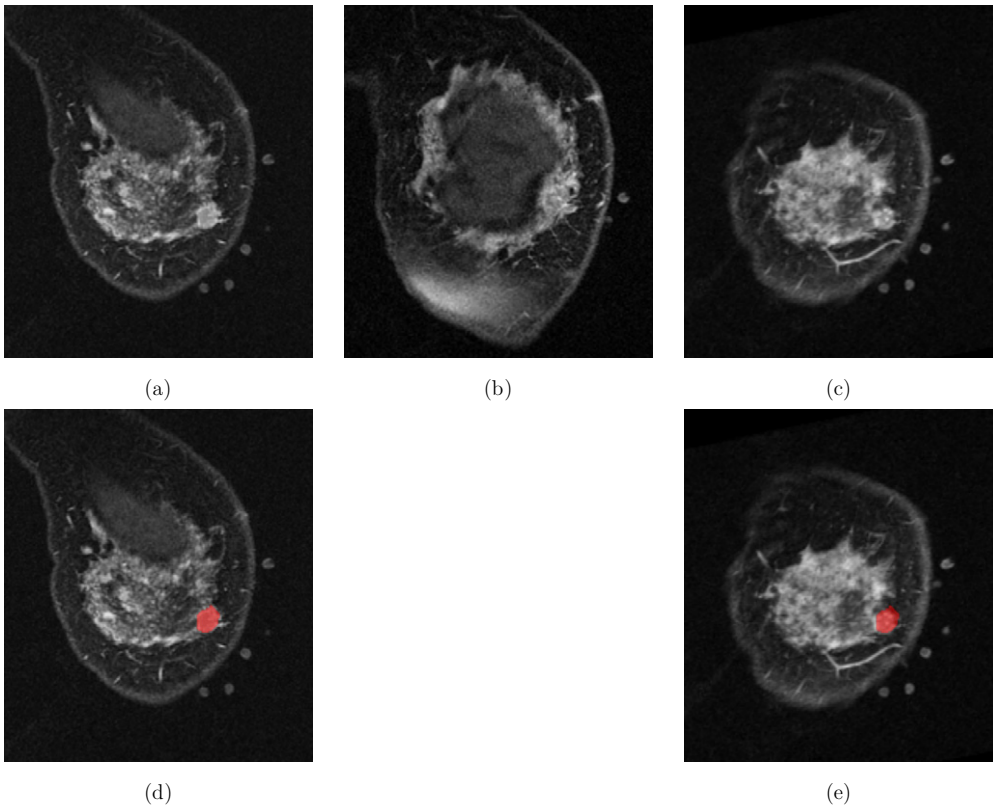

Figure 3. Images with (a) the arm adjacent to the body (reference) and (b) the arm placed above the head (arm up). Result of the registration of the arm up to the reference (c). Segmented tumour in the reference image (d) shown in red and as a colour-overlay on the registered image (e).

dataset was manually verified to ensure the reliability of the tuned parameters. We then employed the same set of parameters on our patient dataset.

To further enhance the accuracy of the matching, we also eliminated the markers which were found to be outliers, see (Chui and Rangarajan 2003). The number of matched markers are presented in the fourth column of table 1. In the matching process of the markers where there was an ambiguity between the markers with high proximity we eliminated those to avoid possible misregistration. The ambiguity was calculated using the correspondence matrix M described in the matching algorithm (Chui and Rangarajan 2003). If there was no element with a value of over 90% in a column of M, the marker corresponding to that column was eliminated. In the case of patient 2, there were 5 markers out of the 29 that were eliminated from the arm up position in the matching process. It should be noted that in the practical application of the scheme, marker matching will be performed by an optical tracking system.

2.4. Tumour segmentation

Three independent observers, all of whom were experienced in looking at breast MR images, segmented the tumours of each of the patients using TurtleSeg (Interactive 3D

Table 2. Evaluating Dice measure of overlap among three tumour segmentations A, B, C, for each patient and arm position.

	P1 D	P1 U	P2 D	P2 U	P3 D	P3 U	P4 D	P4 U	P6 D	P6 U
Seg A and Seg B	92	86	87	82	93	92	90	75	90	86
Seg A and Seg C	93	84	83	80	93	92	87	72	81	82
Seg B and Seg C	91	88	83	80	95	89	88	77	82	84
Average	92.0	86.0	84.3	80.7	93.7	91.0	88.3	74.7	84.3	84.0

Table 3. Evaluating COM variations among three tumour segmentations A, B, C, for each patient and arm position in millimeters.

	P1 D	P1 U	P2 D	P2 U	P3 D	P3 U	P4 D	P4 U	P6 D	P6 U
Seg A and Seg B	0.6	1.9	0.6	0.8	0.8	0.6	0.2	1.5	0.2	0.6
Seg A and Seg C	0.5	1.9	1.1	1.0	1.2	1.8	0.7	1.4	3.6	1.2
Seg B and Seg C	1.1	0.8	1.6	0.4	0.7	2.0	0.7	0.8	3.7	1.0
Average	0.73	1.53	1.10	0.73	0.90	1.46	0.53	1.23	2.50	0.93

Image Segmentation Software)[5] that provides a semi-manual tool for segmentation. Table 1 summarizes the mean ± standard deviation of the segmented tumour volumes. The tumour of patient no. 3 could not be reliably identified and segmented even with the help of a radiologist therefore we segmented an enhancing cyst that was clearly visible in the images instead. Here, we present data for five of the patients from our study named as patient 1, 2, 3, 4, and 6.

3. Results

3.1. TPS registration results on the datasets

By performing the TPS registration scheme on the data and employing all of the selected markers we obtain the registered arm up image. The registration results for a slice of the first and the sixth patient datasets are displayed in figures 2, 3. It can be visually observed that the internal structures of the 'arm up' and the 'arm down' images correspond well.

3.2. Validating the TPS registration

We evaluated the Dice measure of overlap defined as $\text{Dice}(A, B) = 100 \times \frac{2\|A \cap B\|}{\|A\|+\|B\|}$ among three tumour segmentations A, B, C, for each patient and arm positions given in table 2. These numbers indicate the degree of overlap among different segmentations. Furthermore, we evaluated the centre of mass (COM) variations computed as the standard deviation of the COM among these three tumour segmentations, for each patient and arm position in millimeters, given in table 3.

In the next step, we computed the Dice measure of overlap between the tumour in the reference and the registered arm up images presented in table 4(a).

In addition, we computed the COM of the tumours and evaluated the Euclidean distance between the tumours in the reference and arm up images; this is defined as the COM-displacement. We compared the COM-displacements calculated from the unregistered image volumes, the volumes registered using simple translations only, and volumes registered using

[5] TurtleSegInteractive 3D Image Segmentation Software www.turtleseg.org

Table 4. (a) Evaluating the Dice measures of tumour overlap, and (b) COM-displacement of tumours in millimeters before and after registration. Three values in each cell represent the values calculated based on each of the three independent tumour segmentations. The maximum possible number of available matched markers have been used which is different for each patient.

Patient ID	Unregistered	Translated	TPS registered
	(a) Dice score (%)		
1	28	61	77
	24	62	79
	20	58	74
2	0	47	75
	0	45	63
	0	48	57
3	26	63	75
	23	60	74
	27	58	77
4	0	0	20
	0	0	23
	0	0	21
6	6	71	61
	10	73	59
	6	73	59
	(b) COM-displacement (mm)		
1	17.8	7.7	2.7
	18.5	7.8	3.0
	19.5	8.7	4.0
2	33.1	8.2	0.9
	33.0	8.8	1.5
	32.4	7.7	2.2
3	31.6	11.5	9.0
	32.2	11.6	9.3
	30.3	12.6	7.9
4	46.8	17.9	8.5
	46.7	17.2	8.3
	46.1	16.7	8.5
6	11.0	2.6	3.9
	10.9	2.6	4.2
	11.2	2.4	5.2

the deformable TPS scheme presented in table 4(b). For our limited patient study, it can be observed that TPS deformable registration performs better than shifting the images using a rigid translation scheme. More details on cases of our patient study will be presented in the summary of results section 3.5.

3.3. Varying the number of markers used

We examined the effect of changing the number of markers used in the TPS registration on the COM-displacement and Dice measure of overlap for the patients, see figure 4 relating

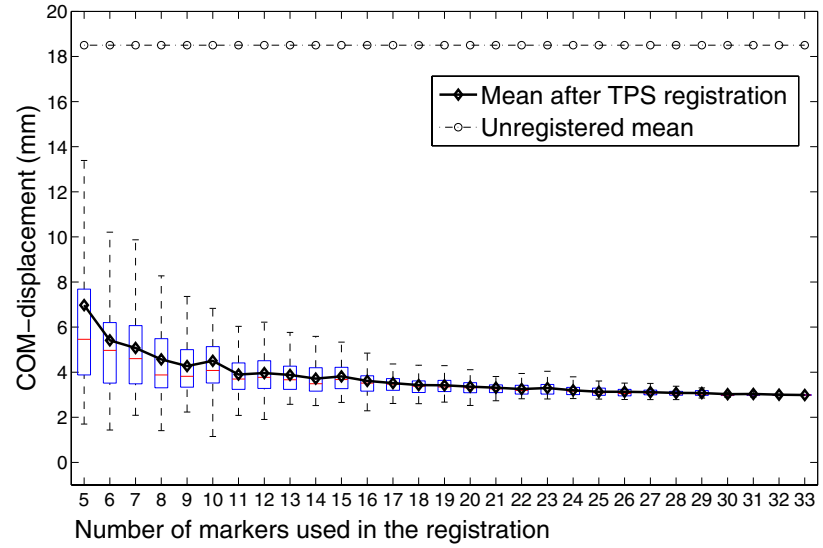

(a)

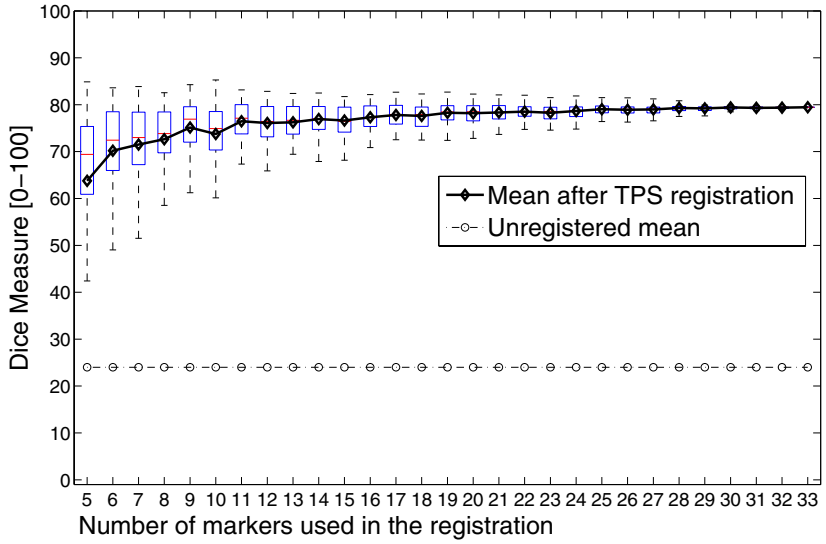

(b)

Figure 4. Studying the effect of changing the number of markers used in the TPS registration for patient 1 on (a) COM-displacement in mm, and on (b) the Dice measure of tumour overlap. Dashed line indicates the mean COM-displacement/Dice before the registration and the solid line shows the mean COM-displacement/Dice for 100 TPS registration experiments. On each box, the central mark is the median, the edges of the box are the 25th and 75th percentiles, and the whiskers extend to the most extreme data points not considered outliers in the registration experiments.

to patient 1. In this experiment, 100 registration experiments were performed for each fixed number of random markers changing from 5 to 33 (for patient 1). Similarly, we compared the mean COM-displacement/Dice varying the number of markers used for all of the patients in figure 5. All of these experiments used tumour segmentation B as an arbitrary choice.

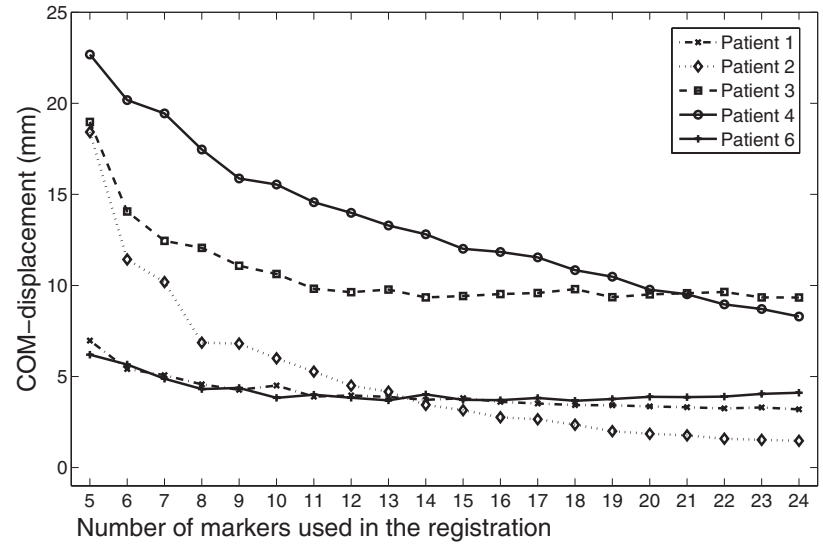

(a)

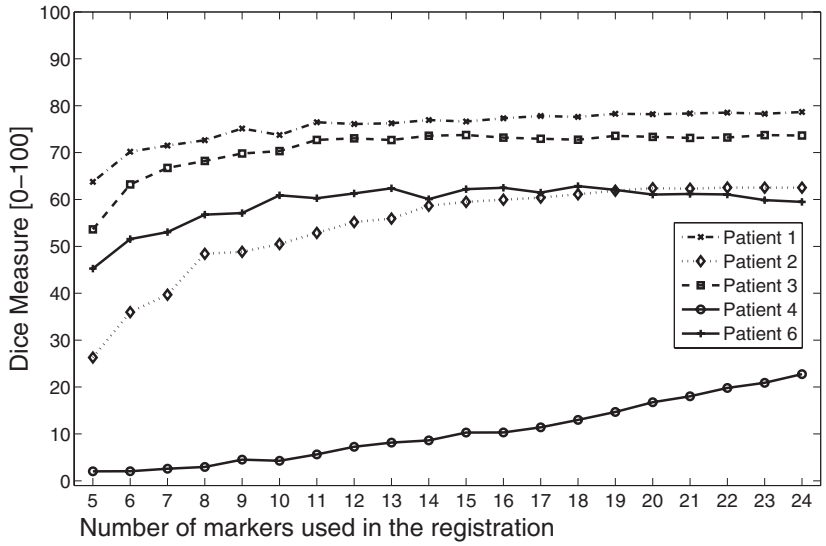

(b)

Figure 5. Studying the effect of changing the number of markers used in the TPS registration on (a) COM-displacement in mm, and on (b) the Dice measure of tumour overlap. Mean COM-displacement/Dice for 100 TPS registration experiments and for each patient is displayed.

3.4. Registration experiments for a fixed number of markers used

We chose subsets of 20 markers 1000 times for all patient datasets and performed the TPS registration for each subset. For the 5 patients 1,2,3,4, and 6, a total of 5000 registration experiments were performed. Figure 6 displays the scatter plot of mean pair-wise Euclidean distance of markers versus registration error measured as the COM-displacement and the scatter plot of mean Euclidean distance of markers to the COM of the tumour versus registration error

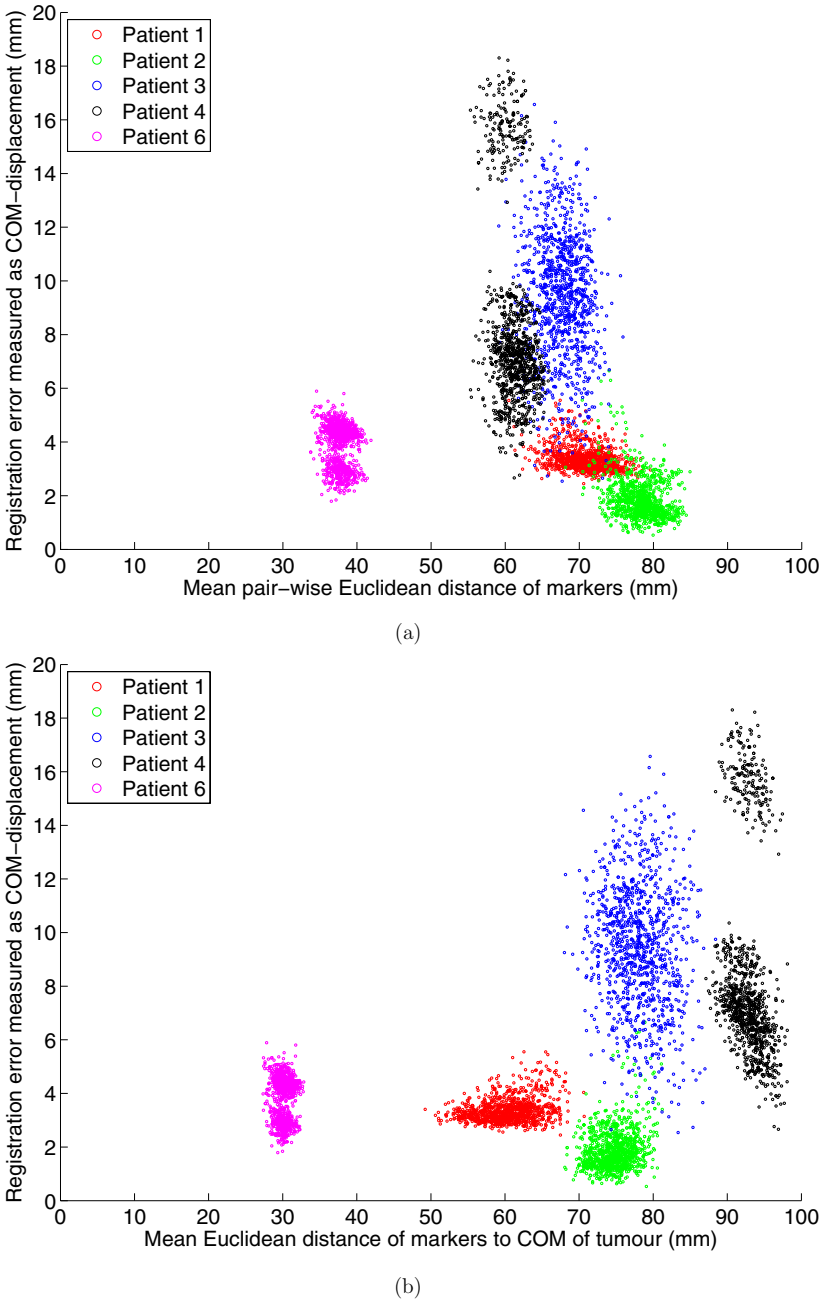

Figure 6. (a) Scatter plot of mean pair-wise Euclidean distance of markers (mm) versus registration error measured as the COM-displacement and (b) scatter plot of mean Euclidean distance of markers to the COM of the tumour (mm) versus registration error measured as the COM-displacement.

measured as the COM-displacement. Figure 7 includes the scatter plot of mean pair-wise Euclidean distance of markers versus the Dice measure of tumour overlap, and the scatter plot of mean pair-wise Euclidean distance of markers versus the Dice measure of tumour overlap.

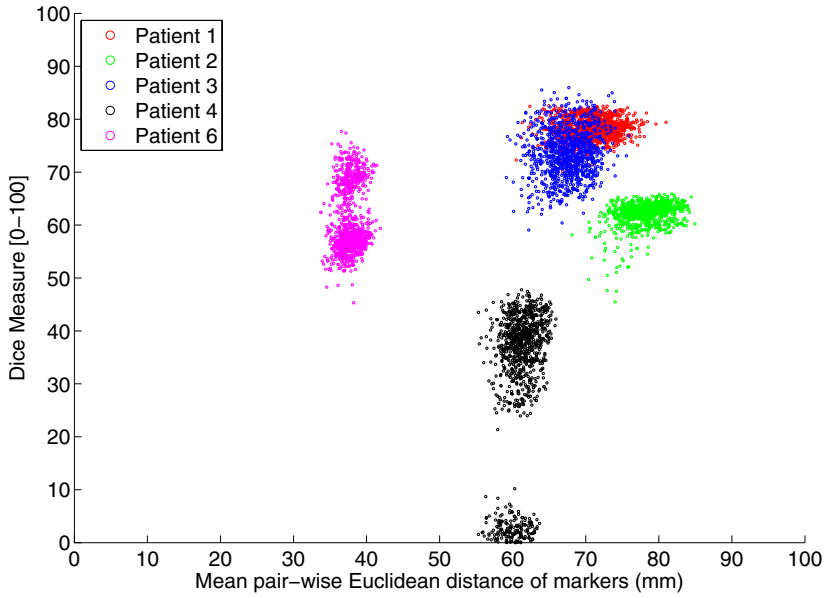

(a)

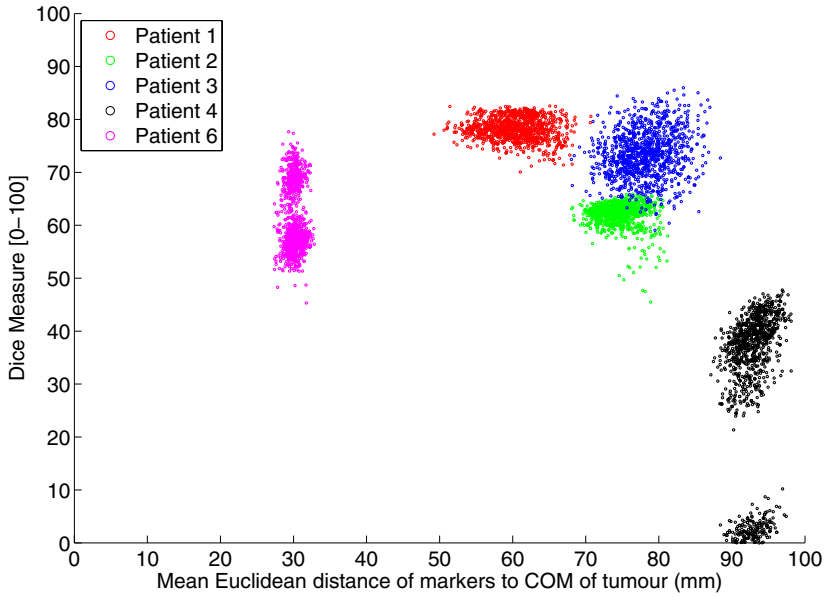

(b)

Figure 7. (a) Scatter plot of mean pair-wise Euclidean distance of markers (mm) versus the Dice measure of tumour overlap and (b) scatter plot of mean Euclidean distance of markers to the COM of the tumour (mm) versus the Dice measure of tumour.

3.5. Summary of results

The focus of this study is the matching of supine breast data-sets which were acquired with two different arm positions using the TPS algorithm and the positions of surface markers. Our goal was to localize the tumour using the described scheme. The results show that the

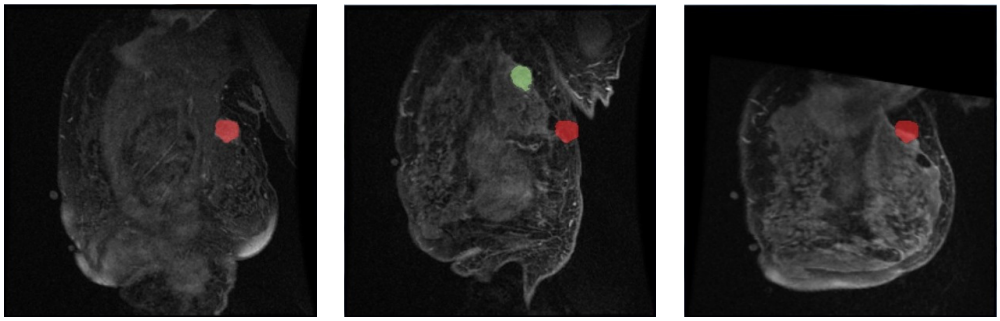

(a) (b) (c)

Figure 8. The registration result for a slice of patient 4. Images with (a) the arm adjacent to the body (reference) and (b) the arm placed above the head (arm up). Result of the registration of the arm up to the reference (c). Segmented tumour in the reference and arm up images are shown respectively in red and green and as a colour-overlay on the registered image.

achievable matching is dependent on the number of markers used for registration. (see figures 4 and 5)

We used manual segmentations of the lesions to assess the DICE overlap and COM-displacement metrics. Figure 2 shows that our interobserver variability was good but the DICE scores were generally slightly lower for the images acquired in the 'Up' position. This reflects the fact that it is more difficult to delineate the lesion boundaries in the second image acquired due to the increased leakage of the contrast agent into the extracellular extravascular space.

It can be observed that Dice measure of patient 4 was not consistent with the other patients in figure 5(b). This could be due to several factors. The initial unregistered arm-up and down positions have a displacement of 46 mm which is the largest among all of the patients in the study.

The registration result for a slice of patient 4 is displayed in figure 8. The attachment of the surface marker has caused a local distortion of the skin surface; this has resulted in a non-physiological local deformation which is not adequately modelled by the TPS. This suggests that trimming the stickers was not sufficient and that an alternative method of attaching the markers to the skin may be needed.

In addition, the segmentation task of the tumour in the arm up position of this patient was also more challenging as reflected by the lower overlap scores in table 2, column (P4 U). This may have been the result of the small size (2.4 cm^3) of the tumour for this patient.

Due to a miscommunication problem in placing the markers, only one side of the breast was covered by the markers for patient 6. In addition, the tumour is close to the COM of the markers and as expected translation gave better results than TPS for patient 6.

The experiments presented in figures 6 and 7 analyse the Dice and COM-displacement measures for a fixed given number of 20 markers. The results presented in this section are consistent with the measurements computed in figure 5 at the location where the number of markers used in the registration is 20. A disparity of the scatter plots relating to patient 4 is visible that can be further explained. The local distortion of the skin surface relating to the data of this patient has caused incorrect marker matching and the registration experiments that have specifically used the incorrectly matched markers lead to poor registration results. The scatter plots relating to patient 6 also exhibit a similar disparity. As explained earlier, markers were placed only on one side of the breast for this patient and the close proximity of

the makers may have led to an incorrect matching. Finally, it can be observed that the scatter plots relating to patient 3 exhibit a wider variation in COM-displacement and Dice measures compared to other patients. Looking at table 1, it can be observed that size of the segmented tumour is significantly larger for this patient. Consequently this can lead to wider variations in registration errors specifically relating to the COM-displacement errors. Note that there is more ambiguity in estimating the COM of a larger tumour than a smaller one, in general, when the tumour boundaries are not precisely known and are semi-manually segmented.

4. Discussion and conclusions

As expected, the result of the experiments vary based on the tumour size, shape, and location. In our patient study, increasing the number of markers decreases the averaged COM-displacement. Although using more markers always improves the quality of registration, it is more difficult to perform the whole registration procedure. More markers will require a longer preparation time. In addition, the localization and identification of each marker in the 3D data-sets gets more challenging.

Based on the experiments presented in this paper we believe using a range of 20 to 30 markers are required for the registration, depending on the breast shape and size. While by decreasing the number of markers we lose registration accuracy, increasing the number of markers might lead to marker matching problems in practice. In addition, proper protocols and communication on the positioning of the markers are required.

We performed experiments on effect of the number of markers used in registration in figures 4 and 5. The graphs in figure 4 relating to patient 1 suggests that no improvement was found in the computed mean COM-displacement and Dice measures beyond the 20 markers.

Our experiments suggest that for a given number of markers, the overall separation of markers (measured as mean pair-wise Euclidean distance of markers) and the mean overall markers' proximity to tumour has no obvious influence on registration quality measures (COM-displacement and Dice) used in this study. More patient datasets with variable breast shape and size and tumour location maybe required to perform solid analysis of the location, distribution, and separation of the markers over the surface and with respect to the tumour.

This was a feasibility study designed to investigate the effect of different arm positions and number of markers on registration accuracy. In order to use a surface marker based registration approach in the surgical setting, further work will be required to optimize the design of the MR-visible markers and the method used to determine their location in the OR.

All MR images in this study were acquired in one breathing stage as gating and tracking of the free breathing motion was performed. As a result, the obtained images were from one point of the respiratory cycle. This is important to obtain a sufficient image quality in the MR images for this study.

During surgery in the OR, breathing motion is expected and has to be addressed. However, other common surgical navigation applications have to address this problem too (for example surgical navigation of spinal cord or brain cases). These use references attached to the object of interest to track motions during the initial stage during registration and then during the rest of the procedure. Most of these techniques are assuming a rigid body (like bone). It is unknown so far, if such a motion tracking approach is efficient in the case of breast surgery. This study cannot answer this question and further studies in the OR will be necessary.

In this study, each registration took under a minute to reconstruct the registered volume in MATLAB on a typical PC. This is important since, for the image-aided BCS, the tracking of the marker positions in the OR and the registration of the supine breast MRI to the OR will be done

while the patient is under anesthesia therefore the registration should be carried out as quickly as possible. An implementation of the TPS algorithm in C could further improve the time efficiency. The speed of the TPS algorithm compared to finite element schemes (Tanner 2005), is an important factor for the clinical application. Another reason to use TPS registration is its simplicity. In general, bio-mechanical models can lead to more accurate tumour localization and can yield superior information about tumour's shape while being more complicated to implement, see (Plewes *et al* 2000) as an example.

It would be also possible to use the registration method to aid ultrasound-guided biopsies (Nakano *et al* 2009). Since both supine breast MRI and ultrasound are performed with the same positioning of the patient, the expected deformations of the breast are even smaller.

In summary we have demonstrated that the alignment of pre-surgical supine MR images to the patient using surface markers on the breast for co-registration is feasible. For BCS, co-registering pre-surgical breast MRI data with the patient positioned as for surgery will provide information on the location, extent and size of a tumour. Current methods of breast tumour localization for surgical excision do not define the tumour perimeter. Negative surgical margins commonly range from less than 1 mm to over 2 cm. Delineation of the tumour perimeter with a less than 5 mm margin of error as described in this study indicates that this registration technique warrants further study as an aid to surgical guidance. Further validation of this approach requires recruitment of more volunteer patients with tumours.

Acknowledgments

This research was supported in part by the Canadian Breast Cancer Foundation and the Terry Fox Foundation for Cancer Research. The authors would like to acknowledge the support of Hologic Inc and the Federal Economic Development Agency for Southern Ontario.

References

Alderliesten T, Loo C, Paape A, Muller S and Gilhuijs K 2010 On the feasibility of MRI-guided navigation to demarcate breast cancer for breast-conserving surgery *Med. Phys.* **37** 2617–26

Bookstein F L 1989 Principal warps: thin-plate splines and the decomposition of deformations *IEEE Trans. Pattern Anal. Mach. Intell.* **11** 567–85

Carter T J, Tanner C, Crum W R, Beechey-Newman N and Hawkes D J 2006 A framework for image-guided surgery *Medical Imaging and Argumented Reality* (*Lecture Notes in Computer Science* vol 4091) ed G-Z Yang *et al* (Heidelberg: Springer) pp 203–210

Carter T, Tanner C, Beechey-Newman N, Barratt D and Hawkes D 2008 MR navigated breast surgery *Medical Image Computing and Computer-Assisted Intervention* (*Lecture Notes in Computer Science* vol 5242) ed D Metaxas *et al* (Heidelberg: Springer) pp 356–363

Chui H and Rangarajan A 2003 A new point matching algorithm for non-rigid registration *Comput. Vis. Image Underst.* **89** 114–41

DeMartini W, Lehman C and Partridge S 2008 Breast MRI for cancer detection and characterization: a review of evidence-based clinical applications *Acad. Radiol.* **15** 408–16

Duchon J 1976 Interpolation des fonctions de deux variables suivant le principe de la flexion des plaques minces *RAIRO Anal. Numer.* **10** 5–12

Goshtasby A A 2005 *2-D and 3-D Image Registration* (New York: Wiley)

Goto M *et al* 2007 Diagnosis of breast tumors by contrast-enhanced MR imaging: comparison between the diagnostic performance of dynamic enhancement patterns and morphologic features *J. Magn. Reson. Imaging* **25** 104–12

Guo Y, Sivaramakrishna R, Lu C C, Suri J S and Laxminarayan S 2006 Breast image registration techniques: a survey *Med. Biol. Eng. Comput.* **44** 15–26

Hajnal J, Hawkes D and Hill D 2001 *Medical Image Registration* (Boca Raton, FL: CRC)

Highnam R and Brady M 1999 *Mammographic Image Analysis (Medical Image Understanding)* (New York: Kluwer)

Konyer N B, Ramsay E A, Bronskill M J and Plewes D B 2002 Comparison of MR imaging breast coils *Radiology* **222** 830–4

Modersitzki J 2004 *Numerical Methods for Image Registration* (New York: Oxford University Press)

Modersitzki J 2009 *FAIR: Flexible Algorithms for Image Registration* (Philadelphia: SIAM)

Nakano S *et al* 2009 Fusion of MRI and sonography image for breast cancer evaluation using real-time virtual sonography with magnetic navigation: first experience *Japan. J. Clin. Oncol.* **39** 552–9

Peters N H, Rinkes I H, Zuithoff N P, Mali W P, Moons K G and Peeters P H 2008 Meta-analysis of MR imaging in the diagnosis of breast lesions *Radiology* **246** 116–24

Piron C A, Causer P, Jong R, Shumak R and Plewes D B 2003 A hybrid breast biopsy system combining ultrasound and MRI *IEEE Trans. Med. Imaging* **22** 1100–10

Plewes D B, Bishop J, Samani A and Sciarretta J 2000 Visualization and quantification of breast cancer biomechanical properties with magnetic resonance elastography *Phys. Med. Biol.* **45** 1591–610

Rohr K 2001 *Landmark-Based Image Analysis (Computational Imaging and Vision)* (Dordrecht: Kluwer)

Scherzer O 2006 *Mathematical Models for Registration and Applications to Medical Imaging* (New York: Springer)

Siegler P, Holloway C M B, Causer P, Thevastasan G and Plewes D B 2011 Supine breast MRI *J. Magn. Reson. Imaging* **34** 1212–8

Tanner C 2005 Registration and lesion classification of contrast-enhanced magnetic resonance breast images *PhD Thesis* University of London

Toga A and Thompson P 2001 The role of image registration in brain mapping *Image. Vis. Comput.* **19** 3–24

Yoo T S 2004 *Insight into Images: Principles and Practice for Segmentation, Registration, and Image Analysis* (*AK Peters Series*) 1st edn (Boca Raton, FL: CRC)